Supporting Information

Eco-friendly synthesis of self-supported N-doped Sb_2S_3-carbon fibers with high atom utilization and zero discharge for commercial full lithium-ion batteries

Hong Yin,[†, §, ‡] Kwan San Hui,[⊥] Xun Zhao,[‡] Shiliang Mei,[§] Xiaowei Lv,[*, †] Kwun Nam Hui,[*, §] Jun Chen[*, ‡]

[†]College of Materials and Chemical Engineering, Key Laboratory of Inorganic Nonmetallic Crystalline and Energy Conversion Materials, China Three Gorges University, Yichang 443002, China

[§]Institute of Applied Physics and Materials Engineering, University of Macau, Avenidada Universidade, Taipa, Macau, China

[‡]Department of Bioengineering, University of California, Los Angeles, Los Angeles, CA 90095, USA

[⊥]School of Mathematics, University of East Anglia, Norwich NR4 7TJ, UK

*Corresponding Authors Email: jun.chen@ucla.edu (J. C.);

bizhui@um.edu.mo (K.N.H.);

xwlv@ctgu.edu.cn (X. L.).

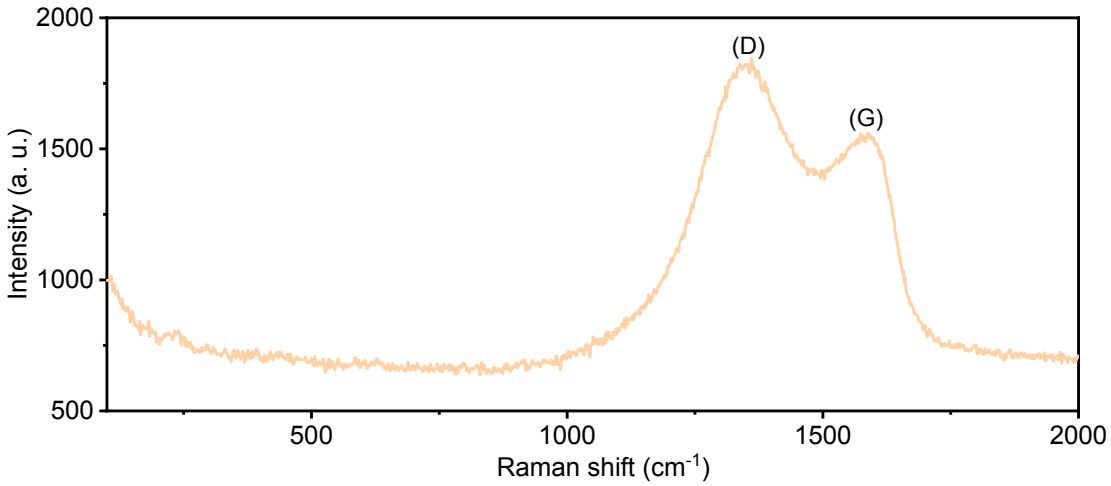

Figure S1. The raman spectra of the N-doped Sb_2S_3 carbon fibers composite.

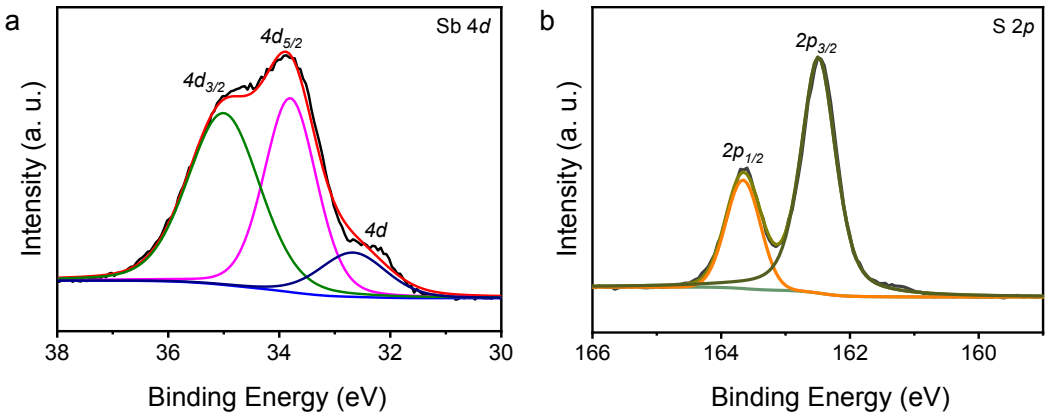

Figure S2. **The XPS spectra of the N-doped Sb_2S_3 carbon fibers composite.** (a), The XPS spectra of Sb 4*d*. (b), The XPS spectra of S 2*p*.

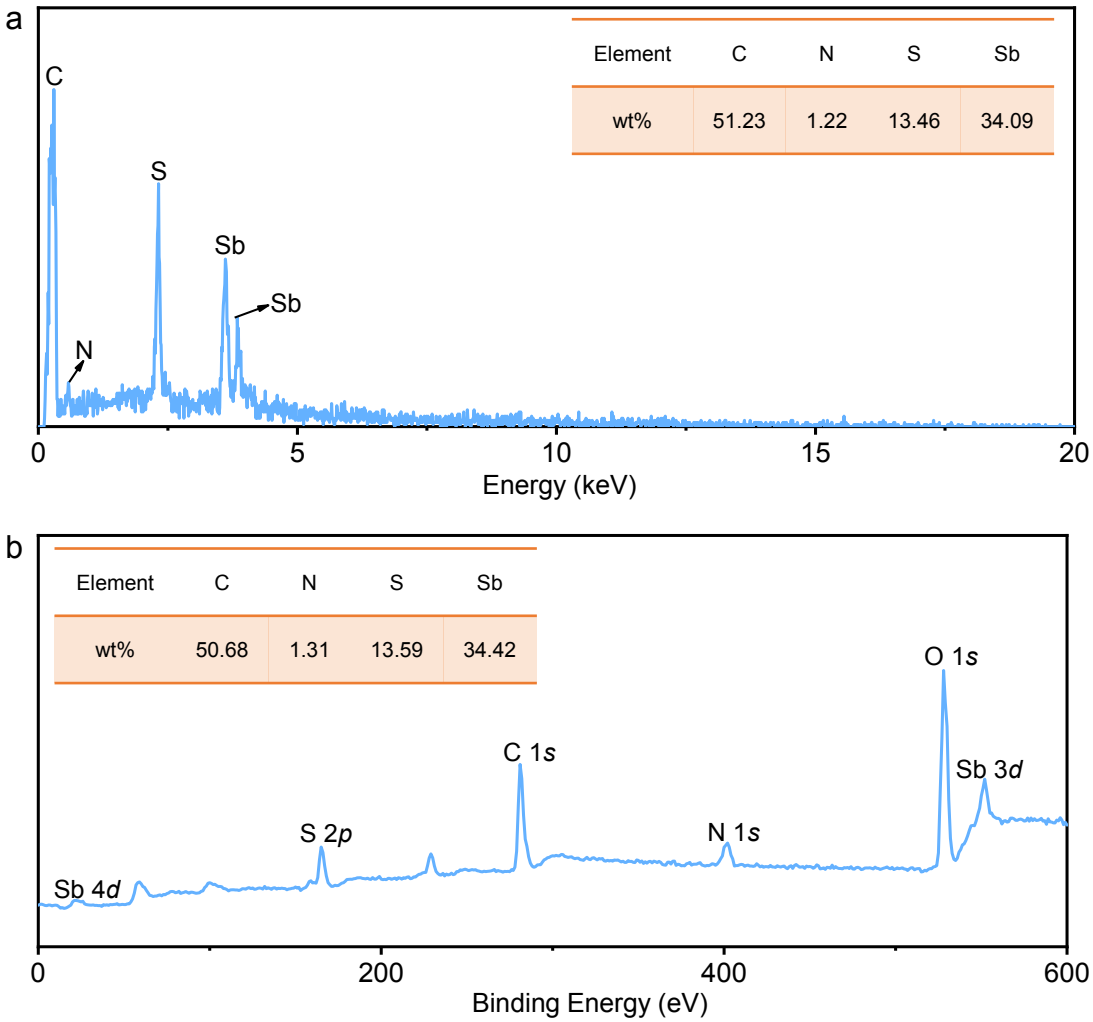

Figure S3. **The quantitative analysis of N, S, and Sb elements in NSSCs composite**. (a), The EDX spectrum of NSSCs composite. (b), The XPS spectrum of NSSCs composite.

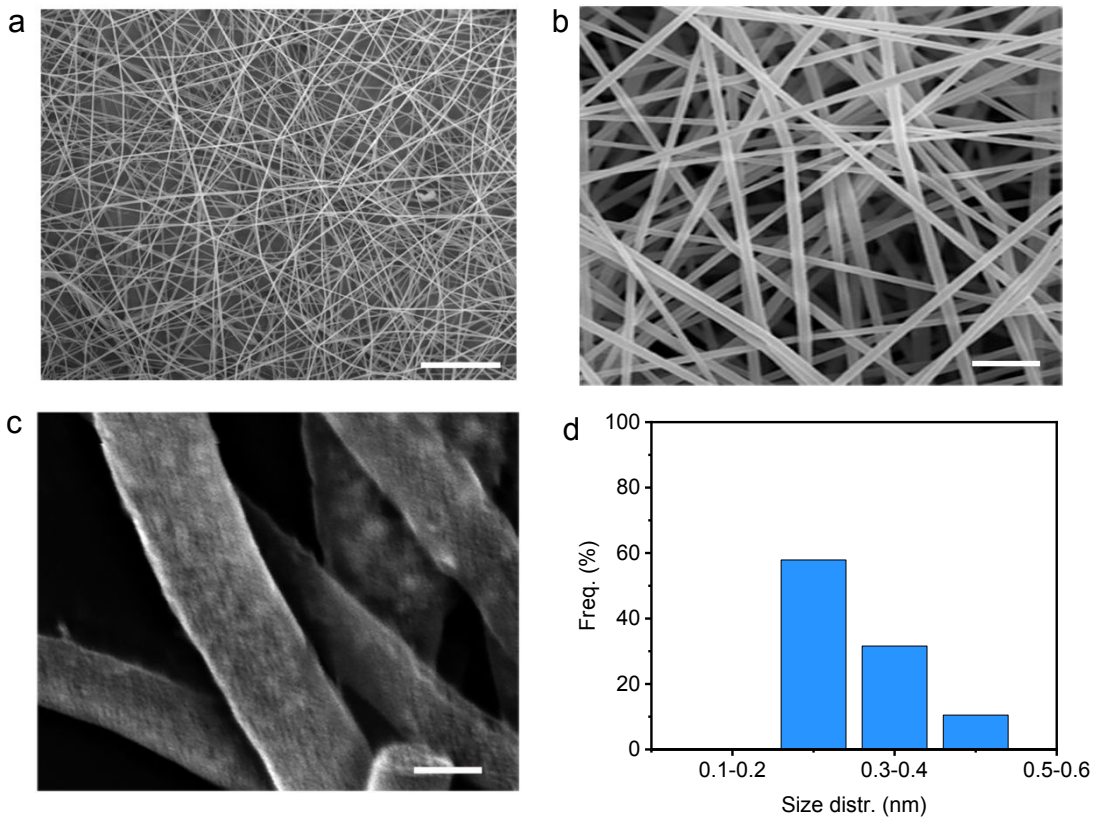

Figure S4. **The size of precursor fiber and Sb_2S_3 nanoparticles in NSSCs composite**. (a), The low magnification SEM image of precursor sample (scale bar, 10 μm). (b), The high magnification SEM image of precursor sample (scale bar, 2 μm). (c), The high magnification of NSSCs composite (scale bar, 100 nm). (d), The size distribution of precursor fibers.

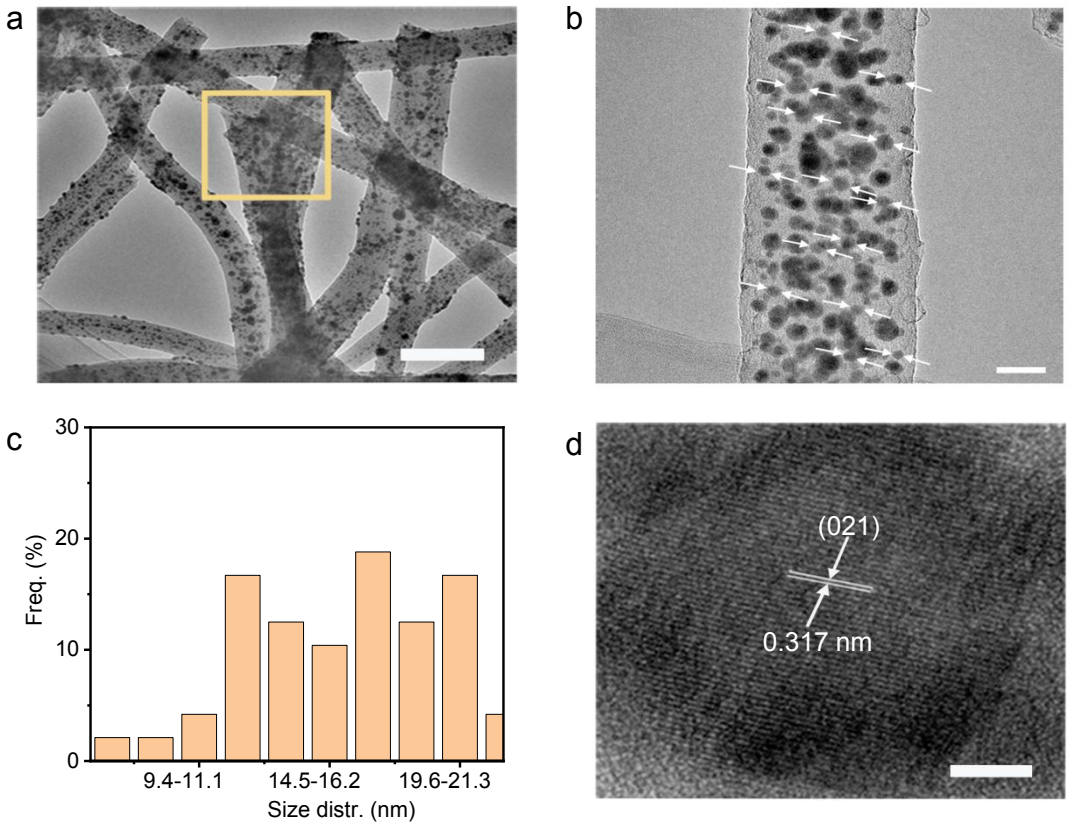

Figure S5. **The TEM images of NCCSs structure**. (a), TEM image of NSSCs nanofiber (scale bar, 200 nm). (b), The high magnification image of NSSCs composite (scale bar, 50 nm). (c), The size distribution of Sb_2S_3 nanoparticles in NSSCs composite. (d), The lattice plane spacing of Sb_2S_3 nanoparticles in NCCSs composite.

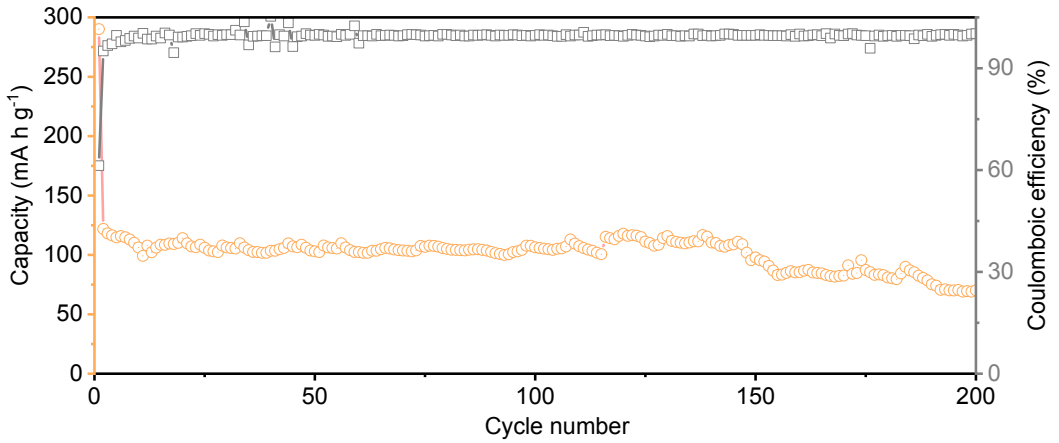

Figure S6. Cycling performance of carbon nanofibers at a cycling rate of 0.2 A g^{-1}.

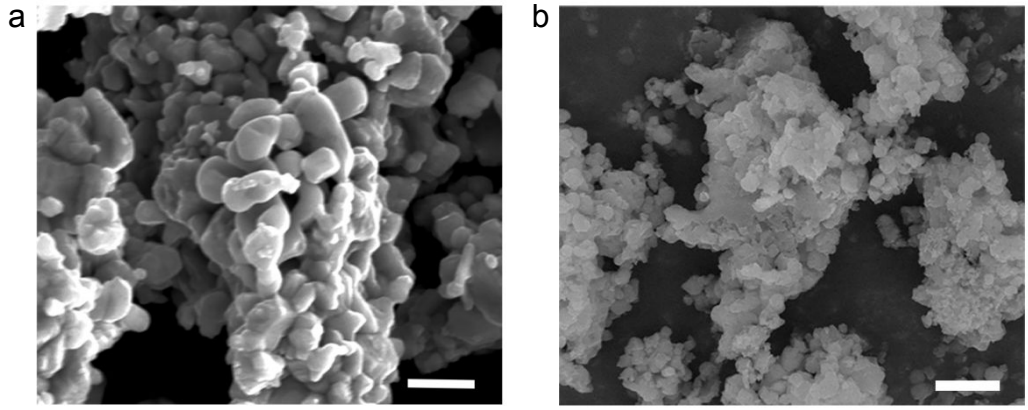

Figure S7. The structure of Sb_2S_3 nanoparticles by high energy ball mill method. (a), SEM images of the as-prepared Sb_2S_3 nanoparticles (scale bar, 1 μm). (b), The cycled SEM image of the SSPs electrode (scale bar, 2 μm).

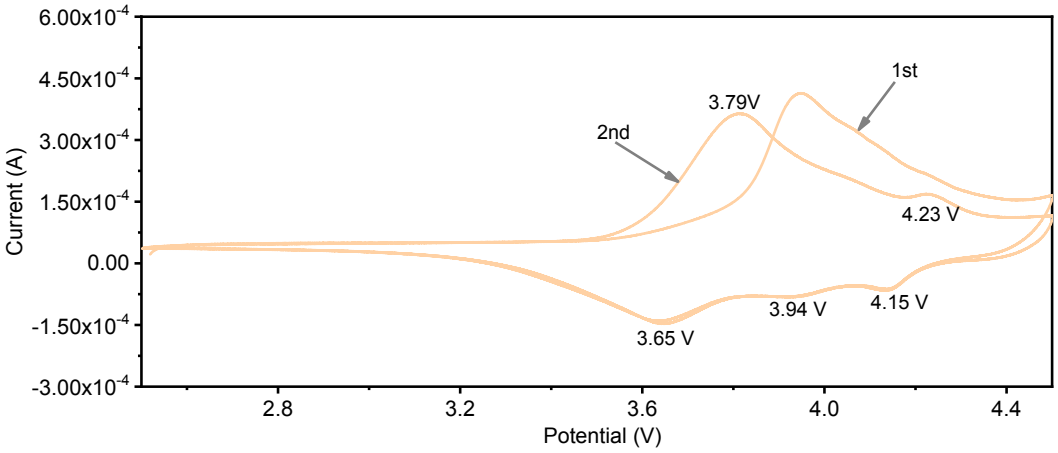

Figure S8. The CV curves of Al_2O_3 coated $LiNi_{0.8}Co_{0.15}Al_{0.05}O_2$ electrode.

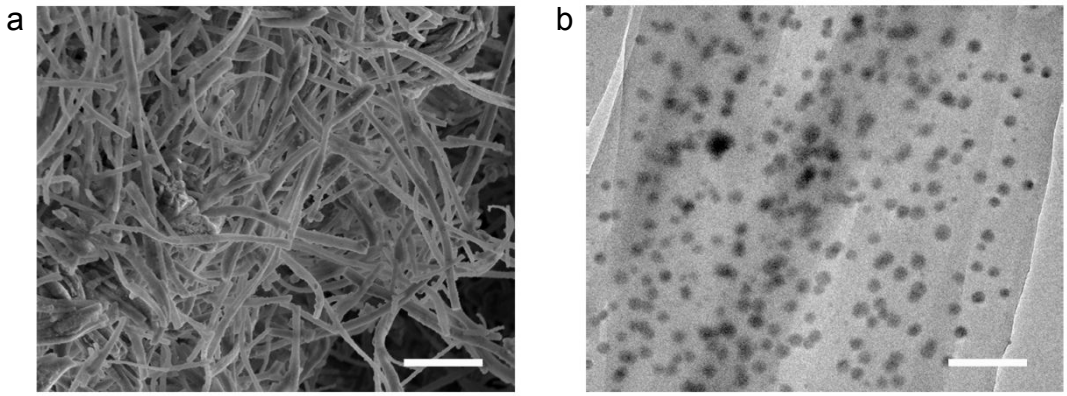

Figure S9. The cycled structure of N-doped Sb_2S_3 carbon fibers electrode after 1000 cycles. (a), The SEM image of NSSCs electrode after cycles (scale bar, 10 μm). (b), The TEM images of NSSCs electrode after cycles (scale bar, 200 nm).

Table S1. Capacitance of Sb_2S_3 storage materials for LIBs prepared by previous works vs our work.

Sample	Current density	Cycles	Capacity (mA h g^{-1})	Ref.
Sb_2S_3/C composite nanorods	100 mA g^{-1}	30	960	1
Sb_2S_3/Sb	100 mA g^{-1}	200	387	2
Bundle-like Sb_2S_3	100 mA g^{-1}	100	548	3
Column-like Sb_2S_3			367	
Nanorod Sb_2S_3	50 mA g^{-1}	25	377	4
Sheaf-like Sb_2S_3			425	
Sb_2S_3@Graphene	50 mA g^{-1}	250	720	5
Sb_2S_3 nanoparticles carbon sphere	100 mA g^{-1}	160	745.3	6
Sb_2S_3/C composite	100 mA g^{-1}	200	435	7
Sb_2S_3/Carbon-silicon nanofibers	200 mA g^{-1}	200	566	8
Rod-like Sb_2S_3/carbon	100 mA g^{-1}	100	591	9
Sb_2S_3 added bio-carbon	100 mA g^{-1}	200	1100	10
Amorphous Sb_2S_3	0.2 C	250	585.4	11
	1000 mA g^{-1} (full cell)	100	467.1	
Sb_2S_3-graphite nanocomposite	200 mA g^{-1}	250	638.2	12
	1000 mA g^{-1}	500	496.1	
Eco-friendly N-doped Sb_2S_3 carbon fibers	**200 mA g^{-1}**	**150**	**606.3**	**This work**
	1000 mA g^{-1}	**1000**	**490.3**	
	0.5 C (full cell)	**200**	**600**	

Supporting note 1.

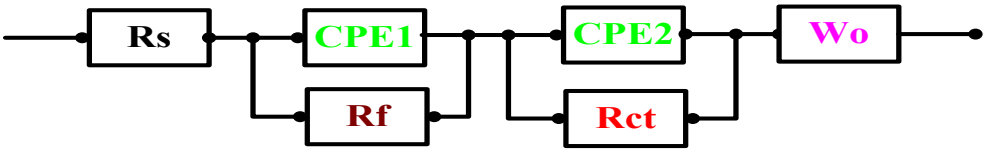

Scheme S1. The equivalent circuit for the NSCCs, SCCs and SSPs electrodes.

The "R_s" represents the solution resistance of the bulk electrolyte, "*CPE*" represents Constant Phase Element, "R_f" represents Li-ion migration resistance, "R_{ct}" represents charge transfer resistance, "W_o-R" represents Warburg Open Circuit Terminus impedance, "W_o-T" represents Open Circuit Terminus T parameter values, "W_o-P" represents Open Circuit Terminus *P* parameter values.[13, 14]

Supporting note 2.

Electric conductivity & Lithium-ion diffusion coefficient at open circuit state,

$$D = R^2T^2/2A^2n^4F^4C^2\sigma^2 \cdots\cdots (1) \qquad Z_{Re} = K + \sigma\omega^{-1/2} \cdots\cdots (2)$$

The "*D"* represents the diffusion coefficient ($cm^2\ s^{-1}$), *R* represents the gas constant (8.31 J $mol^{-1}\ K^{-1}$), "*T"* represents the absolute temperature (298 K), "*A"* represents the surface area of the cathode (0.5 cm^2), "*n"* represents the number of electrons transferred in the half-reaction for the redox couple, "*F"* represents the Faraday constant (96485 C mol^{-1}), "*C"* represents the molar concentration of Li-ions in STNH electrode, *K* represents a constant, "*ω"* represents frequency, and "*σ"* represents the Warburg factor which corresponds to the slope of the curve shown in **Fig. 5d** in the main text.[15-17]

Supporting References:

1. Zhou, X.; Bai, L.; Yan, J.; He, S.; Lei, Z., Solvothermal synthesis of Sb_2S_3/C composite nanorods with excellent Li-storage performance. *Electrochim. Acta* **2013,** *108*, 17-21.

2. Kong, J.; Wei, H.; Xia, D.; Yu, P., High-performance Sb_2S_3/Sb anode materials for Li-ion batteries. *Mater. Lett.* **2016,** *179*, 114-117.

3. Yi, Z.; Han, Q.; Cheng, Y.; Wu, Y.; Wang, L., Facile synthesis of symmetric bundle-like Sb_2S_3 micron-structures and their application in lithium-ion battery anodes. *Chem. Commun.* **2016,** *52* (49), 7691-7694.

4. Ma, J.; Duan, X.; Lian, J.; Kim, T.; Peng, P.; Liu, X.; Liu, Z.; Li, H.; Zheng, W., Sb_2S_3 with various nanostructures: controllable synthesis, formation mechanism, and electrochemical performance toward lithium storage. *Chemistry* **2010,** *16* (44), 13210-13217.

5. Prikhodchenko, P. V.; Gun, J.; Sladkevich, S.; Mikhaylov, A. A.; Lev, O.; Tay, Y. Y.; Batabyal, S. K.; Yu, D. Y. W., Conversion of Hydroperoxoantimonate Coated Graphenes to Sb_2S_3@Graphene for a Superior Lithium Battery Anode. *Chem. Mater.* **2012,** *24* (24), 4750-4757.

6. Luo, W.; Ao, X.; Li, Z.; Lv, L.; Li, J.; Hong, G.; Wu, Q.-H.; Wang, C., Imbedding ultrafine Sb_2S_3 nanoparticles in mesoporous carbon sphere for high-performance lithium-ion battery. *Electrochim. Acta* **2018,** *290*, 185-192.

7. Park, C.-M.; Hwa, Y.; Sung, N.-E.; Sohn, H.-J., Stibnite Sb_2S_3 and its amorphous composite as dual electrodes for rechargeable lithium batteries. *J. Mater. Chem.* **2010,**

20 (6), 1097-1102.

8. Xie, J.; Xia, J.; Yuan, Y.; Liu, L.; Zhang, Y.; Nie, S.; Yan, H.; Wang, X., Sb_2S_3 embedded in carbon-silicon oxide nanofibers as high-performance anode materials for lithium-ion and sodium-ion batteries. *J. Power Sources* **2019,** *435*, 226762.

9. Ru, Q.; Chen, X.; Wang, B.; Guo, Q.; Wang, Z.; Hou, X.; Hu, S., Biological carbon skeleton of lotus-pollen surrounded by rod-like Sb_2S_3 as anode material in lithium ion battery. *Mater. Lett.* **2017,** *198*, 57-60.

10. Mullaivananathan, V.; Kalaiselvi, N., Sb_2S_3 added bio-carbon: Demonstration of potential anode in lithium and sodium-ion batteries. *Carbon* **2019,** *144*, 772-780.

11. Wang, Q.; Lai, Y.; Liu, F.; Jiang, L.; Jia, M., Amorphous Sb_2S_3 Anodes by Reactive RF Magnetron Sputtering for High Performance Lithium-ion Half/Full Cells. *Energy Technol.* **2019,** *7*, 1900928.

12. Liu, Y.; Lu, Z.; Cui, J.; Liu, H.; Liu, J.; Hu, R.; Zhu, M., Plasma milling modified Sb_2S_3-graphite nanocomposite as a highly reversible alloying-conversion anode material for lithium storage. *Electrochim. Acta* **2019,** *310*, 26-37.

13. Fu, Y. S.; Peng, C. Q.; Zha, D. S.; Zhu, J. W.; Zhang, L. L.; Wang, X., Surface pore-containing $NiCo_2O_4$ nanobelts with preferred (311) plane supported on reduced graphene oxide: A high-performance anode material for lithium-ion batteries. *Electrochim. Acta* **2018,** *271*, 137-145.

14. Liao, Y. X.; Li, C.; Lou, X. B.; Hu, X. S.; Ning, Y. Q.; Yuan, F. Y.; Chen, B.; Shen, M.; Hu, B. W., Carbon-coated $Li_3V_2(PO_4)_3$ derived from metal-organic framework as cathode for lithium-ion batteries with high stability. *Electrochim. Acta* **2018,** *271*, 608-

616.

15. Chen, L.; Yang, W. W.; Liu, J. G.; Zhou, Y., Decorating $CoSe_2$ hollow nanospheres on reduced graphene oxide as advanced sulfur host material for performance enhanced lithium-sulfur batteries. *Nano Res.* **2019,** *12* (11), 2743-2748.

16. Jiang, Z. L.; Sun, H.; Shi, W. K.; Zhou, T. H.; Hu, J. Y.; Cheng, J. Y.; Hu, P. F.; Sun, S. G., Co_3O_4 nanocage derived from metal-organic frameworks: An excellent cathode catalyst for rechargeable Li-O_2 battery. *Nano Res.* **2019,** *12* (7), 1555-1562.

17. Kim, H.; Lim, H.; Kim, H. S.; Kim, K. J.; Byun, D.; Choi, W., Polydopamine-derived N-doped carbon-wrapped $Na_3V_2(PO_4)_3$ cathode with superior rate capability and cycling stability for sodium-ion batteries. *Nano Res.* **2019,** *12* (2), 397-404.